

from the same source and that the regular spacing is fortuitous. The temperature and polarization dependence of the 262- and 393-cm<sup>-1</sup> peaks are not the same, indicating that they are not due to the same source. If the 393-cm<sup>-1</sup> peak had a different origin from that of the local resonant-mode peak at 262 cm<sup>-1</sup>, then the higher-wave-number peaks at 525, 660, 785, 918, and 1045 cm<sup>-1</sup> could be considered multiples and combinations of these two vibrations (Table I). In this scheme the spacing of the higher-wave-number peaks would still be approximately 130 cm<sup>-1</sup>.

A possible explanation of the 393-cm<sup>-1</sup> peak is provided by the density of states for the A<sub>1g</sub> mode of the unperturbed CdF<sub>8</sub> complex. There is a broad maximum in the density of states at approximately 380 cm<sup>-1</sup>. In pure CdF<sub>2</sub> the excitation of this peak is not allowed, but it could appear in the doped crystal. This peak appears in the Raman spectrum of only semiconducting CdF<sub>2</sub>: In possibly

because of the large selective enhancement caused by the resonant Raman scattering. By identifying this peak in the A<sub>1g</sub> density of state with the observed peak at 393 cm<sup>-1</sup>, the combinations listed above in Table I are given a plausible basis. The fact that the peak does not fall at 380 cm<sup>-1</sup> could be due to the approximate nature of the calculations used in obtaining the density of states.<sup>6</sup>

Finally, the peak observed at 285 cm<sup>-1</sup> as a shoulder in the semiconducting CdF<sub>2</sub>:0.1-mole% In spectra does not fit into the multiphonon pattern mentioned above. It becomes greatly enhanced in the more highly doped 1.0-mole%-In specimen (Fig. 4). Eisenberger and Adlerstein found a two-phonon peak at 285 cm<sup>-1</sup> which they assigned as the sum of two transverse-optic modes from the (100) symmetry points of the Brillouin zone. The concentration dependence, however, makes more likely the possibility that the 285-cm<sup>-1</sup> band is also a defect vibration.

\*Supported by the Advanced Research Projects Agency under Contract No. DA-49-083.

<sup>1</sup>Present address: Xerox Corporation, Rochester, N. Y.

<sup>1</sup>J. D. Kingsley and J. S. Prener, *Phys. Rev. Lett.* **8**, 315 (1963).

<sup>2</sup>P. F. Weller, *Inorg. Chem.* **5**, 739 (1966).

<sup>3</sup>P. Eisenberger, P. S. Pershan, and D. R. Bosenworth, *Phys. Rev.* **188**, 1197 (1969).

<sup>4</sup>T. H. Lee and F. Moser, *Phys. Rev. B* **3**, 347 (1971).

<sup>5</sup>F. Tautweiler, F. Moser, and R. P. Khosla, *J. Phys. Chem. Solids* **29**, 1869 (1968).

<sup>6</sup>P. Eisenberger and M. G. Adlerstein, *Phys. Rev. B* **1**, 1787

(1970).

<sup>7</sup>I. R. Beattie and T. R. Gibson, *J. Chem. Soc. A* 1970, 981 (1970)

<sup>8</sup>R. Loudon, *Adv. Phys.* **13**, 432 (1964).

<sup>9</sup>J. M. Worlock and S. P. S. Porto, *Phys. Rev. Lett.* **15**, 697 (1965).

<sup>10</sup>R. C. C. Leite, J. F. Scott, and T. C. Damen, *Phys. Rev. Lett.* **22**, 780 (1969).

<sup>11</sup>M. V. Klein and S. P. S. Porto, *Phys. Rev. Lett.* **22**, 782 (1969).

<sup>12</sup>A. Kiel and J. F. Scott, *Phys. Rev. B* **2**, 2033 (1970).

<sup>13</sup>M. G. Adlerstein, P. S. Pershan, and B. J. Feldman, *Phys. Rev. B* **4**, 3402 (1971).

## Energy Bands of Metallic VO<sub>2</sub><sup>†</sup>

Ed Caruthers, Leonard Kleinman, and H. I. Zhang\*

*Department of Physics, University of Texas, Austin, Texas 78712*

(Received 2 October 1972)

At 68 °C, VO<sub>2</sub> undergoes a phase transition from a semiconductor with monoclinic structure to a rather poor metal with the rutile structure. We have performed a modified-augmented-plane-wave (APW) calculation for the metal phase, using a semiempirical potential chosen to give agreement with the experimentally determined energy difference between the top of the O<sub>2p</sub> band and the Fermi surface. A tight-binding parametrized linear-combination-of-atomic-orbitals calculation was fitted to the three points in the Brillouin zone where APW energy levels were calculated, and the resultant energy bands and density of states are presented. Our results indicate that the poor conductivity is due to the flatness of the lower *d* bands (and perhaps correlation effects) and not to any semimetallic nature of the energy bands. We also discuss the molecular-orbital picture of rutile TiO<sub>2</sub> and VO<sub>2</sub>.

### I. INTRODUCTION

Vanadium dioxide is one of a class of transition-metal oxides and sulfides in which an abrupt change in electrical conductivity or magnetic susceptibility takes place at a critical temperature.<sup>1</sup> This class

shows a change in crystal symmetry or in cell volume at the same transition temperature. All these materials are characterized by bands of metal *3d* states lying below the metal *4s* bands and above the oxygen *2p* bands. In VO<sub>2</sub> all the *2p* bands are filled, and there is one electron per vanadium

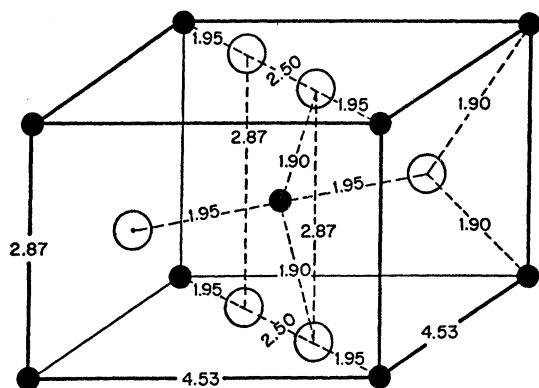


FIG. 1. Unit cell for metallic  $\text{VO}_2$ . The small dark circles are V and the large circles are O. Distances between atoms are given in Å.

atom to go into the  $3d$  bands. There are five  $3d$  levels per vanadium atom and an even number of  $\text{VO}_2$  molecules per unit cell, so it is expected that  $\text{VO}_2$  will be a metal unless one or two  $3d$  bands are completely filled and split off from the rest of the  $3d$  bands.

Above  $68^\circ\text{C}$ ,  $\text{VO}_2$  is a rather poor metal, with about the conductivity of bismuth. At  $68^\circ\text{C}$  there is a phase change and  $\text{VO}_2$  becomes semiconducting. The increase in resistivity may be four orders of magnitude, and is one of the criteria for judging crystal quality.<sup>2</sup> In its high-temperature phase  $\text{VO}_2$  has the rutile structure.<sup>3</sup> The crystal axes are orthogonal, and the primitive lattice translations are  $a\hat{x}$ ,  $a\hat{y}$ , and  $c\hat{z}$ , where  $a=4.530 \pm 0.009$  Å and  $c=2.869 \pm 0.006$  Å. The unit cell contains two formula weights of  $\text{VO}_2$ . If we take one of the vanadium atoms as our origin, then the other vanadium atom is at  $(\frac{1}{2}a, \frac{1}{2}a, \frac{1}{2}c)$  and the four oxygen atoms are at  $(u, u, 0)$ ,  $(-u, -u, 0)$ ,  $(\frac{1}{2}a - u, \frac{1}{2}a + u, \frac{1}{2}c)$ , and  $(\frac{1}{2}a + u, \frac{1}{2}a - u, \frac{1}{2}c)$ , where  $u = 0.305a$ . It is easiest to visualize this system as a body-centered prism, with linear  $\text{VO}_2$  molecules at the corners and the center. The corner  $\text{VO}_2$  molecules are all oriented in the direction from  $(-1, +1, 0)$  to  $(+1, -1, 0)$ . But the molecules in the centers of the prisms are rotated  $90^\circ$  with respect to those at the corners. This structure is shown in Fig. 1.<sup>2</sup> It should be noted that each metal atom has six oxygen neighbors, and that the nearest neighbors to the central vanadium atom are actually the four at  $(\frac{1}{2}a - u, -\frac{1}{2}a + u, \frac{1}{2}c)$ ,  $(\frac{1}{2}a - u, -\frac{1}{2}a + u, -\frac{1}{2}c)$ ,  $(-\frac{1}{2}a + u, \frac{1}{2}a - u, \frac{1}{2}c)$ , and  $(-\frac{1}{2}a + u, \frac{1}{2}a - u, -\frac{1}{2}c)$  belonging to corner molecules. The space group for the rutile structure is  $D_{4h}^{14}(P4_2/mmm)$ . The 16 symmetry operations have been correctly listed by Gay, Albers, and Arlinghaus,<sup>4</sup> who also present the irreducible representations for the various points and lines of high symmetry.

In Fig. 2 we show the Brillouin zone with the points of high symmetry labeled according to Koster's notation.<sup>5</sup>

The above information on the structure and group theory of metallic  $\text{VO}_2$  is in principle sufficient for a first-principles energy-band calculation. But we are forced to introduce further experimental information into our calculation in order to fit experimental results because a self-consistent calculation is computationally impossible due to the low symmetry and large size of the unit cell. Unfortunately, the information below is less reliable than that listed above. For while x-ray diffraction could be done on powder samples or sintered bars, fairly large single crystals are needed for optical or electrical measurements. It is not yet possible to produce large single crystals which are very pure or very free of defects. For example, Ladd<sup>2</sup> reports 70% variations between samples for some reflectivity measurements below the transition temperature. The difficulties are increased by the crystals' tendency to crack when they are cycled through the phase transition. Photoemission from a polycrystalline film of metallic  $\text{VO}_2$  has been studied by Powell, Berglund, and Spicer.<sup>6</sup> According to their measurement, the top of the  $2p$  band is 2.6 eV below the Fermi level. They also concluded that the width of the  $2p$  bands is about 3 eV. But lack of sharpness in their energy distribution curves kept them from being able to locate the bottom of the  $3d$  band. They concluded only that the filled portion of the band is not very narrow, and that it might even overlap the  $2p$  bands. Optical measurements have been made by Verleur, Barker, and Berglund<sup>7</sup> on both single crystals and thin films. They interpret their results in terms of a band scheme in which the  $2p$  bands are separated by about 2.5 eV from the Fermi surface. In anal-

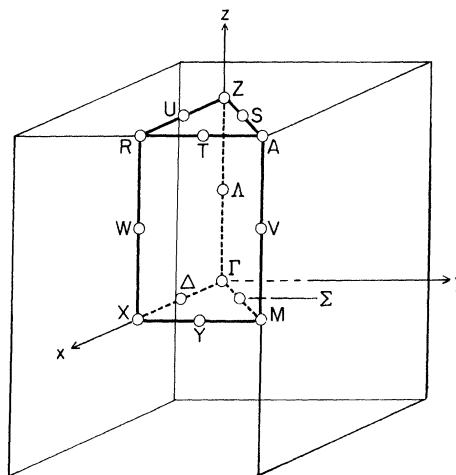


FIG. 2. Brillouin zone for the rutile structure.

ogy to Kahn and Leyendecker's band calculation for SrTiO<sub>3</sub>,<sup>8</sup> flat bands were assumed. Then the high-temperature phase of VO<sub>2</sub> is pictured as a semimetal with one almost filled 3*d* band slightly overlapping the higher-energy 3*d* bands. Verleur *et al.* concluded that this would be consistent with their previous Hall-effect measurement<sup>9</sup> of  $\sim 2 \times 10^{21}$  quasifree electrons per cm<sup>3</sup> (about  $\frac{1}{20}$  the number of electrons which should occupy the 3*d* bands). Ladd<sup>2</sup> analyzed similar optical results and also did a calculation in the effective-mass approximation, using a simple two-band model. He also concluded that the distance from the Fermi surface to the top of the 2*p* bands is about 2.5 eV. But his calculation yielded a *p-d* band gap of about 1.3 eV, with a Fermi energy near the center of the 3*d* bands. Ladd noted that since the effective-mass approximation is not valid in this case, the Hall relationship  $R_H = -1/ne$  is not valid, and  $n$  cannot be computed. He considered it more reasonable to assume that each vanadium ion contributes one conduction electron, and that  $R_H$  is greater or less than  $-1/ne$  depending on the shape and properties of the Fermi surface. We consider that the 2.5–2.6-eV difference between the top of the oxygen 2*p* bands and the Fermi surface is experimentally well established, but that all estimates of the band gap depend on band pictures which are necessarily cruder than our own final results. The oxygen-2*p*-Fermi-surface energy difference was held fixed in our calculation letting the band gap fall where it will.

## II. ENERGY BANDS

Since we are not performing a self-consistent calculation, it is necessary to find a semiempirical potential which will bring our results into agreement with known experimental data. We first generated Coulomb potentials and charge distributions for vanadium and oxygen atoms from Herman's numerical program.<sup>10</sup> We chose the radii of our augmented-plane-wave (APW) spheres to be  $r_v = 2.11$  and  $r_o = 1.48$  Bohr radii in order to enclose the largest possible volume (about  $\frac{1}{3}$  of the unit cell) without overlapping. The spherically averaged contributions to the Coulomb potentials and charge distributions inside the APW spheres were calculated using Löwdin's  $\alpha$ -expansion method.<sup>11</sup> We used the Slater free-electron-exchange approximation throughout our calculation<sup>12</sup>:

$$V^{\text{exch}}(r) = -6[3\rho(r)/8\pi]^{1/3}. \quad (1)$$

In addition, we added a constant potential  $V_0$  within the oxygen sphere and  $-V_0$  inside the vanadium sphere to account for ionization and Madelung potentials. These cannot be determined from first principles except by a fully self-consistent calculation. Because of the large size of the unit cell

we found that 350–400 augmented plane waves were needed for the calculation to converge. Therefore it is computationally impossible to achieve self-consistency. This simple parameter was chosen to have the value  $V_0 = 0.100$  Ry to fit the experimental energy difference between the top of the 2*p* bands and the Fermi level.

We have used the warped-muffin-tin-potential modified-APW method of Kleinman and Shurtleff.<sup>13</sup> In this method, the potential outside the APW spheres only contributes to the matrix elements through its Fourier transforms. The Coulomb contribution to the Fourier transforms was calculated directly from the atomic Coulomb potentials. The exchange contribution was obtained by assuming that all charge not contained in the APW spheres is distributed uniformly in the interstitial region. Using this semiempirical warped-muffin-tin potential, we have calculated the energy eigenvalues at the  $\Gamma$ ,  $Z$ , and  $A$  points in the Brillouin zone. By integrating the associated eigenfunctions we have found the fractions of the electrons which are within the APW spheres and their distribution by orbital symmetry. Table I shows the eigenvalues at  $\Gamma$ , the irreducible representations with which they are associated, and their hybridization. Note that the  $\Gamma_5^+$  levels are doubly degenerate, as are all levels at  $Z$  and  $A$ . Also note that there is substantial *p-d* hybridization between levels at the top of the 3*d* bands and levels at the bottom of the 2*p* bands. Thus the states just above and below the band gap do not interact strongly. The hybridization at  $Z$  and  $A$  is similar to that at  $\Gamma$ .<sup>14</sup>

We have extended these APW results throughout the Brillouin zone by a tight-binding-approximation linear-combination-of-atomic-orbitals (LCAO) calculation. This method starts with atomic orbitals  $\phi_n(\vec{r} - \vec{R}_{\nu m})$ , where  $\vec{R}_{\nu m}$  denotes the position of the  $m$ th atom in the  $\nu$ th unit cell. Bloch functions,

$$\psi_{nmk} = N^{-1/2} \sum_{\nu} e^{i\vec{k} \cdot \vec{R}_{\nu m}} \phi_n(\vec{r} - \vec{R}_{\nu m}), \quad (2)$$

are constructed and the matrix elements become

$$\langle \psi_{jmk} | \hat{H} | \psi_{j'm'k} \rangle = \sum_{\nu} e^{-i\vec{k} \cdot (R_{0m} - R_{\nu m'})} \times \langle \phi_j(r - R_{0m}) | \hat{H} | \phi_{j'}(\vec{r} - \vec{R}_{\nu m'}) \rangle, \quad (3)$$

where the sum runs over all unit cells. In our calculation we only include those values of  $\nu$  and  $m$  which give nearest- or second-nearest-neighbor V-V interactions, nearest- or second-nearest-neighbor V-O interactions, or nearest-, second-nearest-, or third-nearest-neighbor O-O interactions. We also follow the suggestion of Slater and Koster<sup>15</sup> in separating each integral on the right side of (3) into a sum of geometric factors times adjustable parameters. These parameters represent pure  $\sigma$ -,  $\pi$ -, or  $\delta$ -type bonds between neigh-

TABLE I. APW eigenvalues and fraction of electrons with  $s$ ,  $p$ , or  $d$  symmetry inside the APW spheres of vanadium or oxygen at  $k=(0, 0, 0)$ .

| IR           | $E$ (Ry) | Vanadium |        |        | Oxygen |        |        |
|--------------|----------|----------|--------|--------|--------|--------|--------|
|              |          | $s$      | $p$    | $d$    | $s$    | $p$    | $d$    |
| $\Gamma_4^+$ | 0.2372   | 0.0613   | 0.0000 | 0.1698 | 0.0046 | 0.0000 | 0.0333 |
| $\Gamma_5^+$ | -0.0428  | 0.0000   | 0.1052 | 0.0000 | 0.0771 | 0.0420 | 0.0204 |
| $\Gamma_1^+$ | -0.3925  | 0.0648   | 0.0000 | 0.0218 | 0.2001 | 0.0001 | 0.0008 |
| $\Gamma_1^+$ | -0.4958  | 0.0046   | 0.0000 | 0.6744 | 0.0014 | 0.2895 | 0.0008 |
| $\Gamma_5^-$ | -0.5527  | 0.0000   | 0.0000 | 0.6945 | 0.0000 | 0.2588 | 0.0049 |
| $\Gamma_2^+$ | -0.6966  | 0.0000   | 0.0000 | 0.7933 | 0.0000 | 0.1578 | 0.0000 |
| $\Gamma_4^+$ | -0.7009  | 0.0032   | 0.0000 | 0.8732 | 0.0508 | 0.0242 | 0.0048 |
| $\Gamma_5^-$ | -0.8115  | 0.0000   | 0.0000 | 0.9111 | 0.0000 | 0.0000 | 0.0049 |
| $\Gamma_3^+$ | -0.8195  | 0.0000   | 0.0000 | 0.8626 | 0.0000 | 0.0317 | 0.0036 |
| $\Gamma_4^+$ | -0.8316  | 0.0237   | 0.0000 | 0.7596 | 0.0026 | 0.0736 | 0.0082 |
| $\Gamma_1^+$ | -0.8518  | 0.0000   | 0.0000 | 0.8695 | 0.0001 | 0.0118 | 0.0080 |
| $\Gamma_3^+$ | -1.0143  | 0.0000   | 0.0000 | 0.0330 | 0.0000 | 0.7704 | 0.0001 |
| $\Gamma_5^+$ | -1.0279  | 0.0000   | 0.0074 | 0.0000 | 0.0000 | 0.7971 | 0.0000 |
| $\Gamma_1^-$ | -1.0511  | 0.0000   | 0.0212 | 0.0000 | 0.0000 | 0.7939 | 0.0001 |
| $\Gamma_4^-$ | -1.1355  | 0.0000   | 0.0437 | 0.0000 | 0.0000 | 0.7181 | 0.0000 |
| $\Gamma_5^+$ | -1.1768  | 0.0000   | 0.0448 | 0.0000 | 0.0017 | 0.6548 | 0.0002 |
| $\Gamma_5^-$ | -1.2528  | 0.0000   | 0.0000 | 0.2827 | 0.0000 | 0.5385 | 0.0014 |
| $\Gamma_2^+$ | -1.3393  | 0.0000   | 0.0000 | 0.1274 | 0.0000 | 0.4548 | 0.0001 |
| $\Gamma_1^+$ | -1.3455  | 0.0018   | 0.0000 | 0.3028 | 0.0007 | 0.4862 | 0.0002 |
| $\Gamma_4^+$ | -1.3797  | 0.0812   | 0.0000 | 0.1022 | 0.0045 | 0.5044 | 0.0004 |
| $\Gamma_5^+$ | -2.2214  | 0.0000   | 0.0335 | 0.0000 | 0.7828 | 0.0000 | 0.0000 |
| $\Gamma_4^+$ | -2.2558  | 0.0090   | 0.0000 | 0.0467 | 0.7744 | 0.0014 | 0.0003 |
| $\Gamma_1^+$ | -2.3438  | 0.0450   | 0.0000 | 0.0013 | 0.7040 | 0.0006 | 0.0001 |

bors a distance  $|\vec{R}_{0m} - \vec{R}_{\nu m}|$  apart. For metallic  $\text{VO}_2$  we made 12 Bloch sums from the  $2p$  orbitals on the four oxygen atoms in the unit cell, 10 Bloch sums from the  $3d$  orbitals on the two vanadium atoms, two Bloch sums from the  $V_{4s}$  orbitals, and four Bloch sums from the  $O_{3s}$  orbitals. We found that with only these orbitals included, the energy levels at  $Z$  were all the same as those at  $A$ . To break this degeneracy we added eight more Bloch sums, made from the  $d_{xz}$  and  $d_{yz}$  oxygen orbitals. This results in a  $36 \times 36$  complex matrix for a general  $\vec{k}$  point. There are 44 tight-binding parameters, one of which is set permanently to zero because it does not affect any APW eigenvalue. We adjusted these parameters to fit the  $O_{2p}$  levels, the  $V_{3d}$  levels, and the lowest  $s$  level at  $\Gamma$ ,  $Z$ , and  $A$ . We kept the other tight-binding levels above these APW levels.

The fitting was done by an automatic computer

program. The algorithm it uses may be of interest for other problems with many parameters and many levels to fit. Denote the parameters by  $\{p_i\}$ , the tight-binding energy levels by  $\{E_j\}$ , and the APW energy levels by  $\{E_{j0}\}$ . One parameter at a time is changed from  $p_i$  to  $p_i + \Delta_i$ , and all the  $E_j$  to  $E_j + \Delta E_j$ . Small  $\Delta_i$  is assumed, so that  $\partial E_j / \partial p_i \approx \Delta E_j / \Delta_i$ . It is assumed that the  $E_j$  vary linearly near  $p_i$ , so that

$$E_j' = E_j(p_i + \delta p_i) = E_j(p_i) + (\delta p_i) \frac{\partial E_j}{\partial p_i}. \quad (4)$$

An improvement,  $p_i' = p_i + \delta p_i$ , is found by minimizing

$$\sum_j (E_j' - E_{j0})^2 = \sum_j [E_j + (\delta p_i) (\Delta E_j / \Delta_i) - E_{j0}]^2. \quad (5)$$

Setting the derivative with respect to  $\delta p_i$  to zero, one obtains

TABLE II. Tight-binding eigenvalues and hybridization at  $\vec{k}=(0, 0, 0)$ .

| IR           | E (Ry)  | Vanadium |        | Oxygen |        |        |
|--------------|---------|----------|--------|--------|--------|--------|
|              |         | 4s       | 3d     | 3s     | 2p     | 3d     |
| $\Gamma_1^+$ | -0.3767 | 0.750    | 0.199  | 0.0032 | 0.0404 | 0.0000 |
| $\Gamma_5^-$ | -0.5418 | 0.0000   | 0.728  | 0.0000 | 0.271  | 0.0007 |
| $\Gamma_1^+$ | -0.5469 | 0.197    | 0.512  | 0.0027 | 0.274  | 0.0000 |
| $\Gamma_4^+$ | -0.6910 | 0.0072   | 0.974  | 0.0001 | 0.0207 | 0.0000 |
| $\Gamma_2^+$ | -0.7093 | 0.0000   | 0.957  | 0.0000 | 0.0412 | 0.0000 |
| $\Gamma_5^-$ | -0.8170 | 0.0000   | 0.965  | 0.0000 | 0.0201 | 0.0070 |
| $\Gamma_1^+$ | -0.8230 | 0.0233   | 0.955  | 0.0004 | 0.0184 | 0.0000 |
| $\Gamma_3^+$ | -0.8291 | 0.0000   | 0.953  | 0.0000 | 0.0446 | 0.0000 |
| $\Gamma_4^+$ | -0.8303 | 0.0141   | 0.970  | 0.0001 | 0.0148 | 0.0000 |
| $\Gamma_3^+$ | -1.0132 | 0.0000   | 0.0446 | 0.0000 | 0.954  | 0.0000 |
| $\Gamma_1^-$ | -1.0346 | 0.0000   | 0.0000 | 0.0000 | 1.00   | 0.0000 |
| $\Gamma_5^-$ | -1.0351 | 0.0000   | 0.0000 | 0.0001 | 1.00   | 0.0000 |
| $\Gamma_4^-$ | -1.1053 | 0.0000   | 0.0000 | 0.0000 | 1.00   | 0.0000 |
| $\Gamma_5^-$ | -1.1970 | 0.0000   | 0.0000 | 0.0001 | 1.00   | 0.0000 |
| $\Gamma_5^-$ | -1.2763 | 0.0000   | 0.299  | 0.0000 | 0.700  | 0.0001 |
| $\Gamma_2^+$ | -1.3143 | 0.0000   | 0.0416 | 0.0000 | 0.958  | 0.0000 |
| $\Gamma_1^+$ | -1.3473 | 0.0029   | 0.330  | 0.0001 | 0.668  | 0.0000 |
| $\Gamma_4^+$ | -1.3965 | 0.0026   | 0.0408 | 0.0003 | 0.956  | 0.0000 |

$$\delta p_i = - \left( \sum_j \frac{\Delta E_j}{\Delta_i} (E_j - E_{j0}) \right) / \sum_j \left( \frac{\Delta E_j}{\Delta_i} \right)^2. \quad (6)$$

Since the actual dependence of the energy levels on the tight-binding parameters is highly nonlinear,  $p_i + \delta p_i$  may not actually reduce the sum of squares of differences from the APW energies, and each prediction must be checked before improvement of the next parameter is begun. With 42 energy levels to be fitted and 43 parameters which could be varied independently, it was possible to fit the APW energies with various sets of bands. We therefore also required that the eigenvectors for the tight-binding eigenvalues at  $\Gamma$ ,  $Z$ , and  $A$  match the APW hybridizations. To do this most efficiently we first optimized the  $p$ - $p$  and  $d$ - $d$  parameters while setting all the  $p$ - $d$  parameters and higher interactions to zero. In the second step the  $p$ - $d$  parameters were added to the set being varied. The final step varied all the parameters without restrictions. If this order is not followed, the interactions between the upper levels which are not being fitted and the  $p$  and  $d$  levels becomes anomalously large. When the hybridization requirement is included, we find that our system is slightly overdetermined. The rms difference between APW eigenvalues and tight-binding eigenvalues is only a little less than 0.02 Ry per eigenvalue. Table II shows the tight-binding eigenvalues at  $\Gamma$ , the irreducible representations with which they are associated, and the charge distribution. In comparing

Tables I and II, it must be kept in mind that Table I refers to electron density within the APW sphere, whereas Table II gives the total electron density associated with atomic wave functions. For example,  $V_{4s}$  functions will have most of their charge concentrated in the interstitial region, or even inside the APW spheres of neighboring oxygen atoms.

Once the parameters have all been fitted, the energy eigenvalues can be found quickly at any point in the Brillouin zone. We have calculated 9072 points (825 of them independent). The energy bands along principal symmetry directions are presented in Fig. 3 and the density of states is shown in Fig. 4. Our bands do not support the assumption<sup>7</sup> that VO<sub>2</sub> is a semimetal. The  $d$  bands are only slightly narrower than those calculated for iron<sup>16</sup> and there is a great deal of band crossing as well as band overlap. We think that the poor conductivity is due to a combination of heavy band mass, many-body interactions, and poor quality of the crystals. [*Note added in proof.* D. B. McWhan, Phys. Rev. B (to be published), finds from specific heat measurements on VO<sub>2</sub> with enough WO<sub>2</sub> added to make it metallic at helium temperatures that  $m^* = 36m_e$ . This large  $m^*$  is due to both band and many-body effects.] The Fermi energy is -0.8158 Ry, about 0.58 eV above the bottom of the conduction band.<sup>17</sup> As a result of our semiempirical potential, the distance from the top of the oxygen 2p bands to the Fermi surface is 2.67 eV. We find that the band gap is indirect with a total width of 2.09 eV between a maximum in the valence band at  $\Sigma$  and a minimum in the conduction band at  $R$ . This, of course, is not a self-consistent calculation. But we do not expect more detailed calculations to give qualitatively different results. In particular, our APW eigenvalues would have to be radically reordered to split one  $d$  band off from the rest. It is difficult to see how the large amount of crossing along interior lines could be removed. In the following paper we will show how to construct semiconducting energy bands for the monoclinic low-temperature phase of VO<sub>2</sub> from the results of the present calculation. The fact that this can be done gives us confidence in the result presented above.

*Note added in proof.* W. E. Spicer (private communication) states that in contradiction to the optical experiments,<sup>7</sup> photoelectric experiments do not allow a  $p$ - $d$  gap anywhere near as large as 2.09 eV. We can easily reduce the size of this gap by increasing  $V_0$ , the ionization and Madelung contribution to the potential, but only at the cost of reducing the  $p$  to Fermi surface gap an equal amount. Spicer would like us to drop the bottom of the  $d$  band, keeping the Fermi level fixed, thus keeping the  $p$  to Fermi level gap fixed while decreasing the  $p$ - $d$  gap. This we do not think can be done with any reasonable crystal potential.

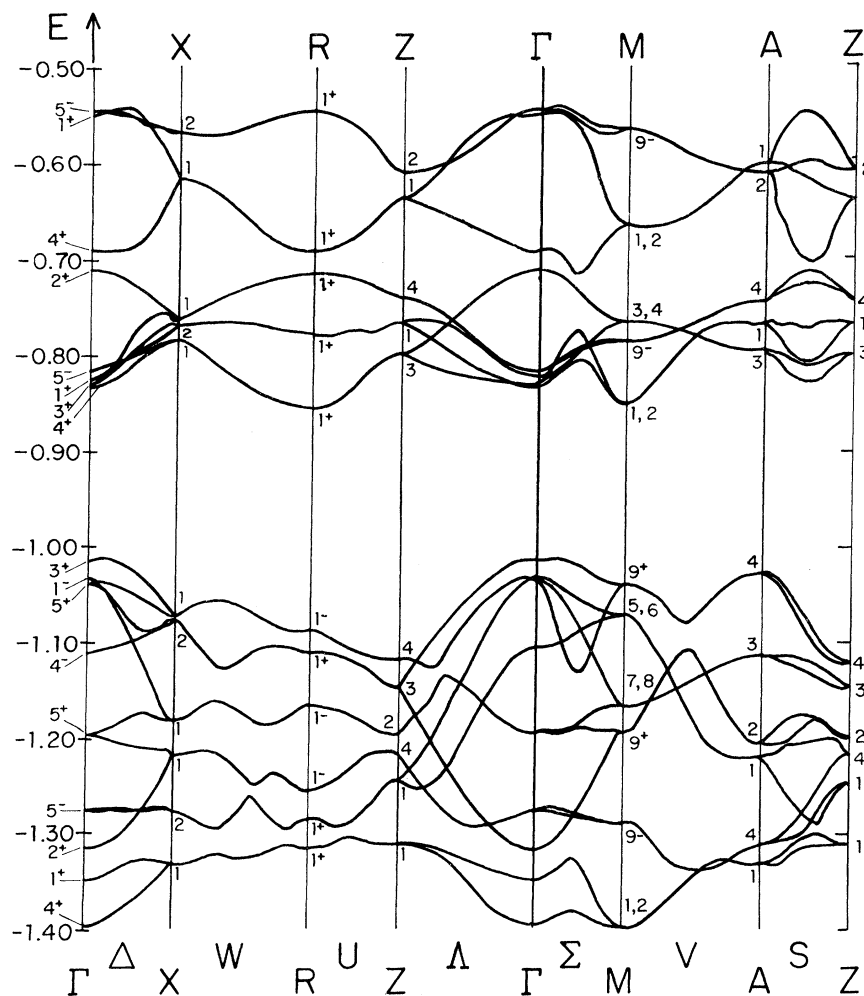


FIG. 3. Energy bands along principal symmetry directions for metallic  $\text{VO}_2$ . Eigenvalues have been labeled at high-symmetry points and symmetries along intermediate directions can be found from a table of compatibility relations.<sup>4</sup> Note that  $M_1$  and  $M_2$ ,  $M_3$  and  $M_4$ ,  $M_5$  and  $M_6$ , and  $M_7$  and  $M_8$  are degenerate pairs by time-reversal symmetry. Energy is in Ry.

### III. DISCUSSION

We would now like to contrast our results with the qualitative pictures of the conduction band which have been derived from the molecular-orbital (MO) theory. This model usually considers only a central cation and its nearest anion neighbors. The rutile structure is replaced by a central metal ion at  $(0, 0, 0)$  and six oxygen ions at  $(\pm u, 0, 0)$ ,  $(0, \pm u, 0)$ , and  $(0, 0, \pm u)$ . The point group for rotations about the central metal ion is  $O_h$ , and molecular orbitals are projected from atomic orbitals according to the various irreducible representations.

Fischer<sup>18</sup> has interpreted his x-ray emission data for  $\text{TiO}_2$  in terms of this model. He replaces the

conduction band by two discrete energy levels—one made up of two  $\sigma$  bonds which transform like  $E_g$ , the other made up of three  $\pi$  bonds which transform like  $T_{2g}$ . The energies of these two levels are determined by decomposing the x-ray absorption spectrum into two Gaussians, each due to a transition from a core level to a conduction level. We would like to point out that even though this model uses two discrete energy levels, we judge from the half-widths of the Gaussians that the bandwidths are about 3 eV for the three  $t_{2g}$   $\pi$  orbitals and 2 eV for the two  $e_g$   $\sigma$  orbitals. This agrees fairly well with our results, though our density of states reveals considerably more structure than was detected by x rays.

A more sophisticated MO model has been pro-

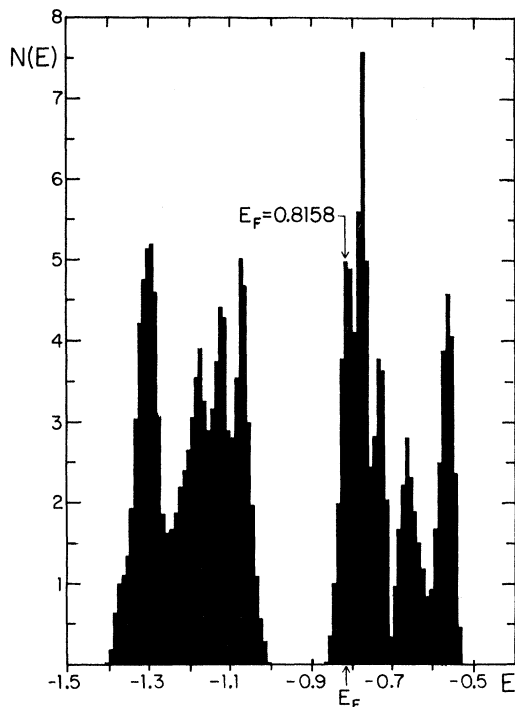


FIG. 4. Density of states of metallic VO<sub>2</sub>. Units along the vertical axis are arbitrary. Energy is in Ry.

posed for rutile VO<sub>2</sub> by Goodenough.<sup>19</sup> The actual symmetry of the crystal is more carefully considered in this theory. For example, the  $\sigma$  molecular orbitals are made up of two  $e_g$  states, the  $\pi$  orbitals are made up of three  $t_{2g}$  states, and it is recognized that distortions in the octahedron of oxygens surrounding the central vanadium atom add an orthorhombic component to the crystal field which splits all degeneracies. Goodenough has also recognized that vanadium atoms are close enough together along the  $c$  axis to bond with each other. In his model the three  $t_{2g}$  levels consist of two  $pd\pi$  antibonding orbitals partially overlapping a cation-to-cation orbital (denoted  $dd_{||}$ ). The bonding  $pd\pi$  states are assumed to occupy the upper portion of the valence bands, while the bonding

and antibonding  $pd\sigma$  states lie at the bottom of the valence band and the top of the conduction band, respectively. Lately Goodenough<sup>19,20</sup> has suggested that the driving force for the metal-semiconductor transition may be increased  $pd\pi$  overlap in the monoclinic phase. This increased overlap would lower the energy of the  $pd\pi$  bonding levels, but the  $pd\pi$  antibonding level would be raised above the  $dd_{||}$  levels. The symmetry change would then split the  $dd_{||}$  levels into completely filled and completely empty bands.

Examination of Table I shows that only levels near the bottom of the valence band or the top of the conduction band are strongly hybridized. For instance, the lowest five valence levels average 51% O<sub>2p</sub>, 22% V<sub>3d</sub>, and 27% interstitial, while the lowest six conduction levels average 85% V<sub>3d</sub>, 3% O<sub>2p</sub>, and 12% interstitial. Clearly, electrons in these latter levels do not participate strongly in  $pd$  covalent bonding. But since the separation between nearest-neighbor vanadium atoms along the  $c$  axis is 3.6 times the radius of a vanadium APW sphere, it is apparent that the lowest conduction levels do not represent  $dd$  covalent bonding either. In fact, the  $pd$  and  $dd$  covalent characters of these levels are roughly equivalent. This was determined by testing the changes produced in the  $\Gamma$ -point eigenvalues by 5% changes in the  $pd\sigma$ ,  $pd\pi$ ,  $dd\sigma$ ,  $dd\pi$ , and  $dd\delta$  parameters. Though the lowest six  $d$  levels are somewhat more affected by changes in  $dd$  parameters than by changes in  $pd$  parameters, changes in the  $pd\pi$  affect four of the six eigenvalues ( $\Gamma_4^+$ ,  $\Gamma_3^+$ ,  $\Gamma_1^+$ , and  $\Gamma_2^+$ ) almost as much as changes in the  $dd$  parameters. Since the nearest-neighbor vanadium-vanadium and vanadium-oxygen distances are sharply reduced in the monoclinic phase, the above analysis shows that both the  $pd\pi$  and the various  $dd$  parameters should be important in opening the semiconducting gap in the low-temperature phase. Actual calculations for the monoclinic phase show that this is the case.<sup>21</sup> Thus Goodenough's model of the transition process is correct, even though covalent bonding is less important for states near the  $p$ - $d$  energy gap in the metallic phase than his MO theory implies.

<sup>1</sup>Research supported by the Air Force Office of Scientific Research (AFSC) under Grant Nos. AF-AFOSR-68-1507 and AF-AFOSR-72-2308.

\*Present address: Department of Applied Physics, College of Engineering, Seoul National University, Seoul, Korea.

<sup>1</sup>D. Adler, *Solid State Phys.* **21**, 1 (1968).

<sup>2</sup>L. Ladd, Office of Naval Research Technical Report Nos. HP-26, and ARPA-41, 1971 (unpublished).

<sup>3</sup>S. Westman, *Acta Chem. Scand.* **15**, 217 (1961).

<sup>4</sup>J. G. Gay, W. A. Albers, Jr., and F. J. Arlinghaus, *J. Phys. Chem. Solids* **29**, 1449 (1968).

<sup>5</sup>G. F. Koster, *Solid State Phys.* **5**, 173 (1957).

<sup>6</sup>R. J. Powell, C. N. Berglund, and W. E. Spicer, *Phys. Rev.* **178**, 1410 (1969).

<sup>7</sup>H. W. Verleur, A. S. Barker, and C. N. Berglund, *Phys. Rev.* **172**, 788 (1968).

<sup>8</sup>A. H. Kahn and A. J. Leyendecker, *Phys. Rev.* **135**, A1321 (1964).

<sup>9</sup>A. S. Barker, Jr., H. W. Verleur, and J. H. Guggenheim, *Phys. Rev. Lett.* **17**, 1286 (1966).

<sup>10</sup>F. Herman and S. Skillman, *Atomic Structure Calculations* (Prentice-Hall, Englewood Cliffs, N. J., 1963).

<sup>11</sup>T. Loucks, *Augmented Plane Wave Method* (Benjamin, New York, 1967).

<sup>12</sup>J. C. Slater, Phys. Rev. **81**, 385 (1951).

<sup>13</sup>L. Kleinman and R. Shurtleff, Phys. Rev. **188**, 1111 (1969).

<sup>14</sup>Tables similar to Table I may be obtained from the authors for the Z and A points.

<sup>15</sup>J. C. Slater and G. F. Koster, Phys. Rev. **94**, 1498 (1954).

<sup>16</sup>R. Shurtleff and L. Kleinman, Phys. Rev. B **3**, 2418 (1972).

<sup>17</sup>In order to avoid confusion when we talk about hybridized *p-d* bands we shall refer to the bands which are  $O_{2p}$  and  $V_{3d}$

in the tight-binding limit as valence and conduction bands, respectively.

<sup>18</sup>D. W. Fischer, Phys. Rev. B **5**, 4219 (1972).

<sup>19</sup>J. B. Goodenough, J. Solid State Chem. **3**, 490 (1971).

<sup>20</sup>J. W. Pierce and J. B. Goodenough, Phys. Rev. B **5**, 4104 (1972).

<sup>21</sup>E. B. Caruthers and L. Kleinman, following paper, Phys. Rev. B **7**, 3760 (1973).

## Energy Bands of Semiconducting $VO_2$ <sup>†</sup>

Ed Caruthers and Leonard Kleinman

*Department of Physics, University of Texas, Austin, Texas 78712*

(Received 30 October 1972)

For  $T > T_t \approx 68^\circ \text{C}$ ,  $VO_2$  is a metal with the rutile structure. For  $T < T_t$ ,  $VO_2$  is a semiconductor with a monoclinic structure. We have found semiconducting energy bands for the low-temperature structure from a parametrized tight-binding linear-combination-of-atomic-orbitals calculation. The semiconducting gap results not only from the reduced symmetry of the monoclinic phase but also from changes in the tight-binding parameters which result from changed interatomic distances. The joint density of states derived from our calculation is in very good agreement with experimental optical data. The success of this calculation shows that, given the crystal structure, the semiconducting band gap is completely understandable in terms of one-electron theory. A short Appendix on the group theory of this structure is included.

### I. INTRODUCTION

$VO_2$  undergoes a first-order phase transition at  $T_t = 68^\circ \text{C}$  from a monoclinic semiconductor ( $T < T_t$ ) to a tetragonal metal ( $T > T_t$ ). Phase transitions characterize several oxides of vanadium, and the general class of transition-metal oxides shows a wide range of magnetic and electrical properties. All these oxides contain a distinct conduction band, arising from metal *nd* atomic orbitals, which is above a valence band of  $O_{2p}$  states and below the band of metal  $(n+1)s$  states. In the case of  $VO_2$ , the  $3d^3 4s^2$  vanadium atoms contribute four electrons each to fill the valence band. This leaves one electron per vanadium ion in the conduction band. Since there are an even number of vanadium atoms in the unit cell ( $V_2O_4$  for  $T > T_t$ ,  $V_4O_8$  for  $T < T_t$ ), the semiconducting state must be characterized by a gap separating completely filled bands of  $3d$  states from all the higher-energy  $3d$  states. A great deal of work has been devoted to the problems of how the band gap arises from the phase transition, and what the mechanism is which drives the transition.<sup>1,2</sup>

In principle the investigation of  $VO_2$  should include completely self-consistent band calculations, using nonspherical potentials, performed on both the high- and low-temperature phases. The detailed energy bands would facilitate interpretation

of optical and photoemission experiments. The differences in the charge density of the two phases would greatly aid explanation of the transition, as would changes in the various components of the binding energy. Unfortunately, this sort of calculation is not technically feasible for  $VO_2$ . The high-temperature phase has a tetragonal unit cell containing two formula weights of  $VO_2$  (rutile structure). In our investigation of this phase<sup>3</sup> we found that the large size of the unit cell relative to the augmented-plane-wave (APW) spheres made 350–400 APWs necessary for the expansion of the wave functions. Since there are 12 filled valence bands and ten conduction bands (five of which are partially occupied), the calculation of charge density necessary for a self-consistent calculation was not possible. The low-temperature phase has a monoclinic space group with four formula weights of  $VO_2$  in the unit cell, and is even less amenable to exact calculation.

The purpose of this paper is to present a first approximation to the energy bands of semiconducting  $VO_2$ . In order to show how the band gap arises from the changes in crystal symmetry, we have performed a parametrized tight-binding linear-combination-of-atomic-orbitals (LCAO) calculation on the monoclinic crystal structure. Our method was to begin with all tight-binding parameters (TBPs) that were the same as those which produced